Talanta 84 (2011) 305–313

Contents lists available at ScienceDirect

Talanta

journal homepage: www.elsevier.com/locate/talanta

Electrochemical determination of L-phenylalanine at polyaniline modified carbon electrode based on β-cyclodextrin incorporated carbon nanotube composite material and imprinted sol–gel film

Yu-fang Hu [a], Zhao-hui Zhang [a,b,*], Hua-bin Zhang [a], Li-juan Luo [a], Shou-zhuo Yao [b]

[a] College of Chemistry and Chemical Engineering, Jishou University, Hunan 416000, PR China
[b] State Key Laboratory of Chemo/Biosensing and Chemometrics, Hunan 410082, PR China

ARTICLE INFO

Article history:
Received 10 October 2010
Received in revised form
22 December 2010
Accepted 6 January 2011
Available online 15 January 2011

Keywords:
Imprinted sol–gel
β-Cyclodextrin incorporated multi-walled carbon nanotube
Polyaniline
Electrochemical sensor
L-Phenylalanine

ABSTRACT

A sensitive and selective electrochemical sensor based on a polyaniline modified carbon electrode for the determination of L-phenylalanine has been proposed by utilizing β-cyclodextrin (β-CD) incorporated multi-walled carbon nanotube (MWNT) and imprinted sol–gel film. The electrochemical behavior of the sensor towards L-phenylalanine was investigated by cyclic voltammetry (CV), differential pulse voltammetry (DPV), and amperometric *i–t* curve. The surface morphologies of layer-by-layer assembly electrodes were displayed by scanning electron microscope (SEM). The response mechanism of the imprinted sensor for L-phenylalanine was based on the inclusion interaction of β-CD and molecular recognition capacity of the imprinted film for L-phenylalanine. A linear calibration plot was obtained covering the concentration range from 5.0×10^{-7} to 1.0×10^{-4} mol L^{-1} with a detection limit of 1.0×10^{-9} mol L^{-1}. With excellent sensitivity, selectivity, stability, reproducibility and recovery, the electrochemical imprinted sensor was used to detect L-phenylalanine in blood plasma samples successfully.

1. Introduction

L-Phenylalanine is an essential amino acid for human and most livestock. It is used widely as food or feed additive in infusion fluids or for chemical synthesis of pharmaceutically active compounds [1,2]. Hyperphenylalaninemia (HPA) serves as the most common inherited disorder of amino acid metabolism and was defined as an increased plasma phenylalanine concentration above 120.0 μmol L^{-1} [3–5]. Although HPA patients show no clinical symptoms during the neonatal period, if undiscovered and untreated during early infancy, the patients will manifest with impaired cognitive development and function leading to mental retardation. Therefore, determination of trace L-phenylalanine in blood plays an important role in clinical medicine.

Molecularly imprinted polymer (MIP) is a synthetic polymer possessing selective molecular recognition properties for the shape and positioning of functional groups. These imprinted materials are similar to biological specific receptors in some ways because of their high selectivity to the target molecule. MIP is a promising material as the recognition element or modifying agent in sensor field [6–10]. However, as a sensing material, one drawback in using the imprinted sensor is that it provides a limited surface area resulted in a very weak electronic signal. Moreover, diffusion of the analytes across the MIP film needs to be accelerated to obtain a quick response [11]. Studies showed that introduction of polyaniline (PAN), β-cyclodextrin (β-CD) or multi-walled carbon nanotubes (MWNTs) nanocomposite materials can improve the overall surface area without substantially changing the size of the electrode and enhance the rate of electron transfer [12,13]. Zhang et al. prepared a series of polyaniline/carbon nanotubes array composite electrodes [14]. Hu et al. synthesized a nanostructure PAN/PAA multilayer film with very stable and higher electrocatalytic ability towards H_2O_2 [15]. Ayad et al. developed a pH sensor based on polyaniline film [16]. These studies indicated that PAN film is an expanding sensitive material to prepare the electrochemical sensor. Carbon nanotube [17–19], a new form of elementary carbon, is composed of graphitic sheets rolled into closed concentric cylinders with diameter of nanometers and length of micrometers. Since the discovery of carbon nanotubes in 1991 [20], they have been attracted wide attention in physical, chemical and material science fields because of their unique characteristic involving high electrical conductivity, chemical stability and mechanical strength. The subtle electronic properties of carbon nanotubes suggest they have the ability to promote electron transfer reaction when used as the electrode material in electrochemical reaction. Meanwhile,

* Corresponding author. Tel.: +86 743 8563911; fax: +86 743 8563911.
E-mail address: zhaohuizhang77@163.com (Z.-h. Zhang).

0039-9140/$ – see front matter © 2011 Elsevier B.V. All rights reserved.
doi:10.1016/j.talanta.2011.01.010

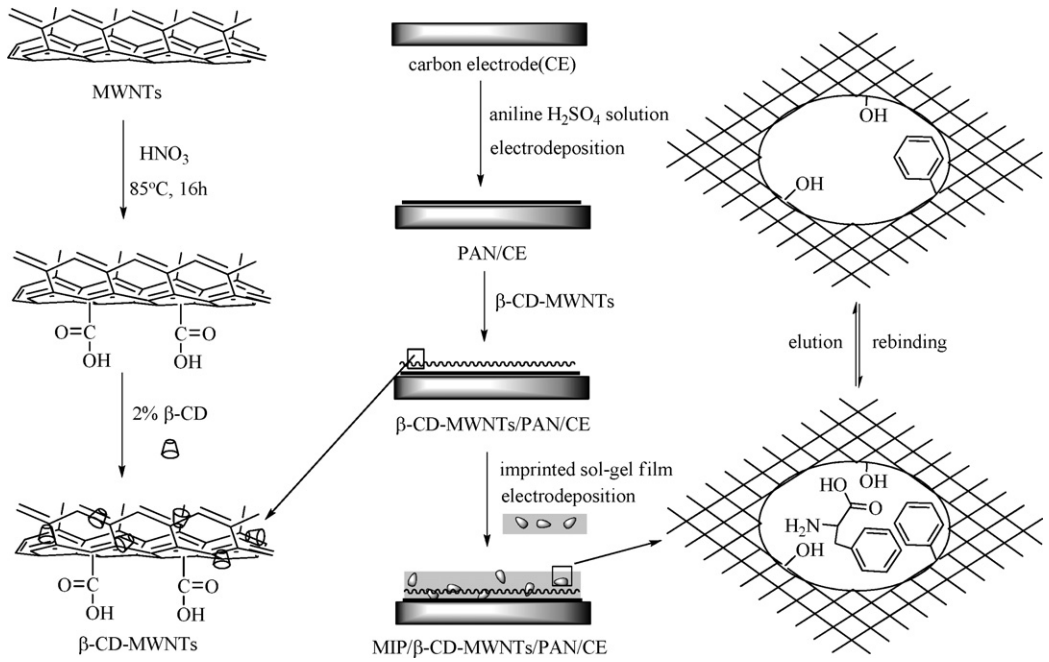

Fig. 1. Illustration of the preparation process of the MIP/β-CD–MWNTs/PAN/CE.

it also provides a new way in the electrode surface modification for designing new electrochemical sensors [21,22] and novel electrocatalytic materials [23]. It has been reported that carbon nanotubes modified electrodes were successfully applied to study and determine many biological and organic molecules [24–26].

Up to now, He et al. prepared an electrochemical sensor for rutin based on β-cyclodextrin incorporated carbon nanotube-modified electrode [27]. On this basis, we explored the value in use of β-cyclodextrin (β-CD) incorporated multi-walled carbon nanotubes (MWNTs) to develop a novel electrochemical imprinted sensor with excellent sensitivity to determine L-phenylalanine. PAN coated electrode with excellent conductivity and stability properties was constructed by electrodepositing aniline solution onto the bare carbon electrode surface. Then, a β-CD incorporated MWNTs (β-CD–MWNTs) modified PAN coated electrode was prepared. The electrochemical behavior of L-phenylalanine at the proposed imprinted sensor was investigated by cyclic voltammetry (CV), differential pulse voltammetry (DPV) and amperometric *i–t* curve. The response mechanism of the sensor for L-phenylalanine

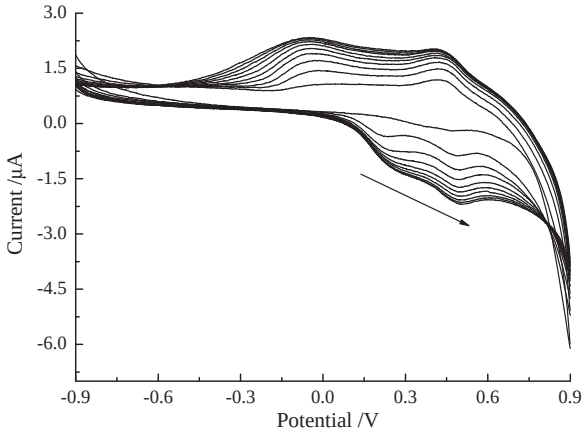

Fig. 2. Cyclic voltammographs of aniline electrodeposition on bare carbon electrode in aqueous solution containing 0.1 mol L^{-1} aniline and 1.0 mol L^{-1} H_2SO_4 at 50 mV s^{-1}, scan time (from inner to outer): 1, 2, 3, 4, 5, 6, 7, 8, 9 and 10.

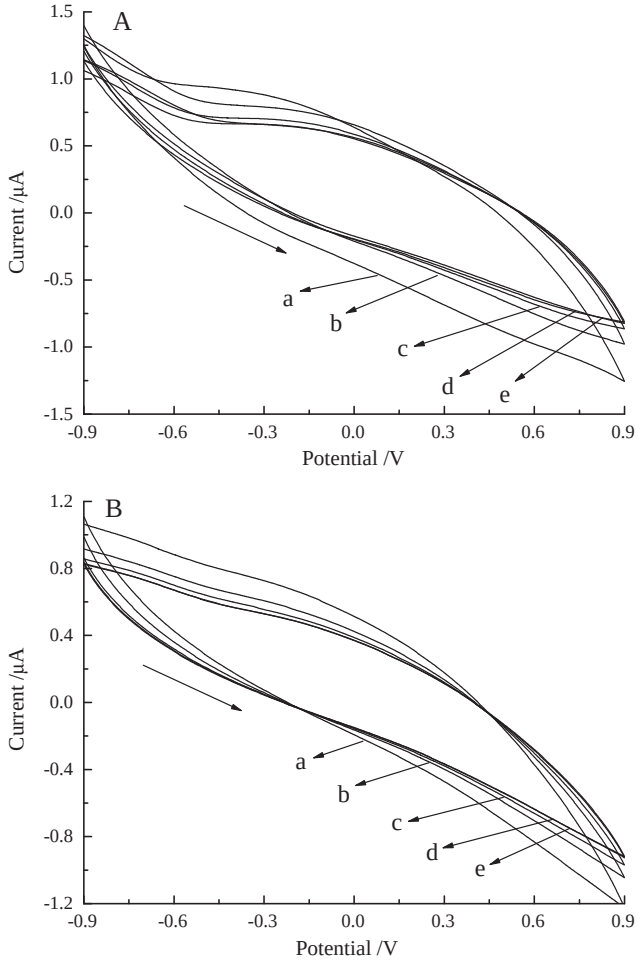

Fig. 3. The cyclic voltammograms of (A) MIP/β-CD–MWNTs/PAN/CE and (B) MIP/CE with a scan rate of 50 mV s^{-1} from −0.9 to 0.9 V. Scan time: (a) 1, (b) 10, (c) 20, (d) 30 and (e) 40.

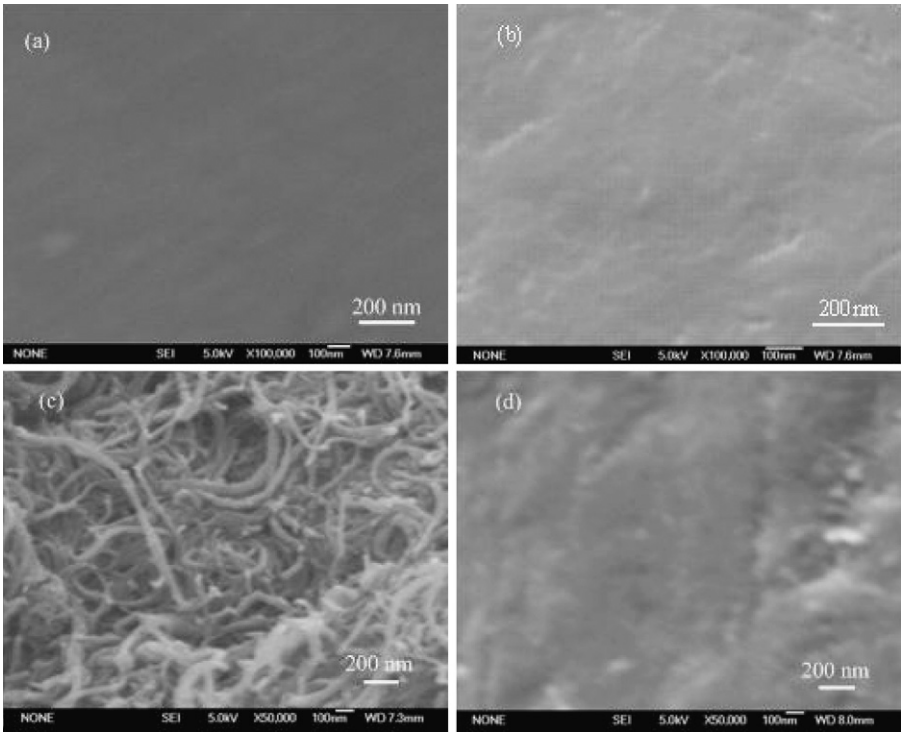

Fig. 4. SEM images of (A) the bare carbon electrode surface, (B) the PAN/CE surface, (C) the β-CD–MWNTs/PAN/CE surface and (D) the MIP/β-CD–MWNTs/PAN/CE surface.

was also discussed. The imprinted electrochemical sensor showed excellent sensitivity, selectivity and stability. It was also employed for the determination of L-phenylalanine in blood plasma samples successfully.

2. Experimental

2.1. Reagents

All the chemicals were of analytical-reagent grade unless otherwise stated and used direct without further purification. The double-distilled water was used throughout this study. Multi-walled carbon nanotubes (MWNTs) with diameters of 20–30 nm were obtained from Shenzhen Technology Company (Guangdong, China). β-Cyclodextrin (β-CD) was purchased from Beijing Aoboxing Biological Technology Company (Beijing, China). Aniline, sulfuric acid and ethoxyethanol were obtained from Changsha Reagent Company (Hunan, China). Methyltrimethoxysilane (MTMOS, 97%), tetraethoxysilane (TEOS) and phenyltrimethoxysilane (PTMOS, 98%) were provided by Sigma (USA). L-Phenylalanine, D-phenylalanine, L-histidine, L-proline, DL-methionine and L-norleucin were obtained from Sigma (USA). All chemical experiments were carried out in phosphate buffer solution (PBS, pH 7.0, 0.2 mol L^{-1}). The buffer solution was prepared by mixing potassium dihydrogen phosphate (KH_2PO_4) and potassium hydrogen phosphate (K_2HPO_4) (Guangdong Jieshan Chemical Plant, China), containing 10.0 mmol L^{-1} potassium ferricyanide ($K_3[Fe(CN)_6]$)/potassium ferrocyanide ($K_4[Fe(CN)_6]$) (1:1).

2.2. Apparatuses and measurements

Electrochemical experiments were performed with a CHI660B electrochemical workstation with a three-electrode system (Shanghai Chenhua Apparatus Company). The modified carbon electrode (CE) was used as working electrode. Platinum wire and saturated calomel electrode (SCE) were used as counter electrode

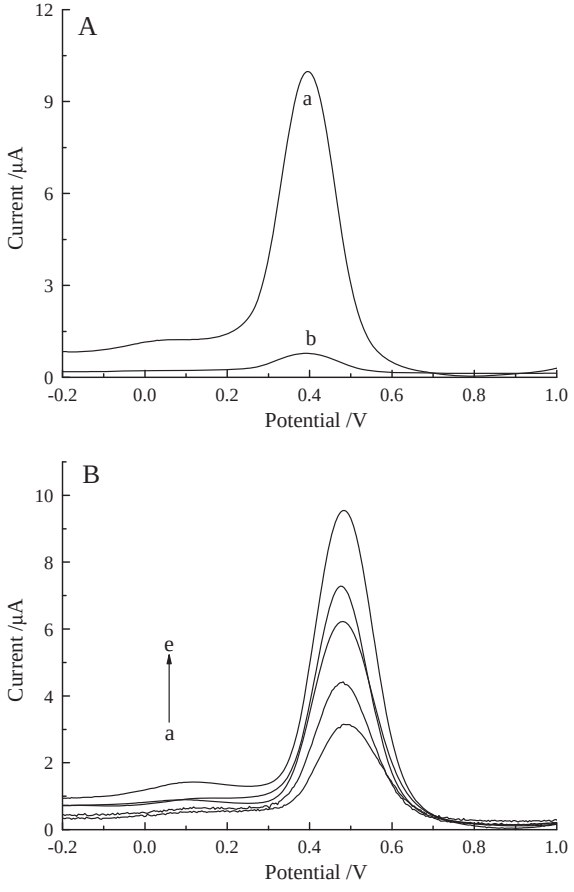

Fig. 5. (A) Typical DPV responses from −0.2 to +1.0 V of the MIP/β-CD–MWNTs/PAN/CE (a) before extraction and (b) after extraction the template molecule; (B) DPV responses of the electrode at different stages in PBS containing 1.0 mmol L^{-1} L-phenylalanine, (a) MIP/CE, (b) MIP/PAN/CE, (c) MIP/MWNTs/PAN/CE, (d) MIP/β-CD–MWNTs/CE and (e) MIP/β-CD–MWNTs/PAN/CE.

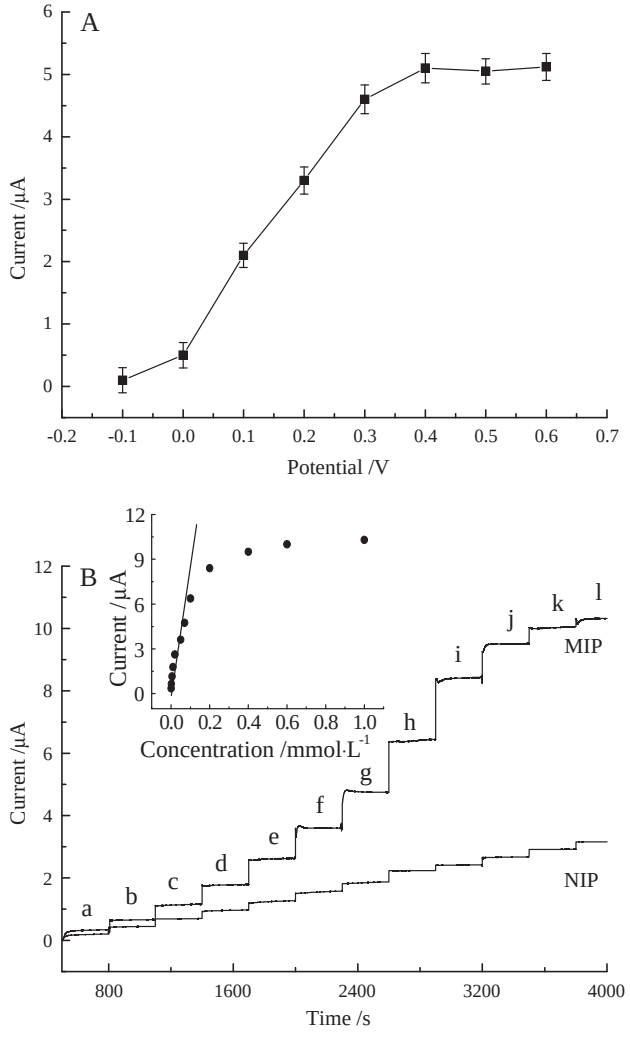

Fig. 6. (A) Polarization curve of MIP/β-CD–MWNTs/PAN/CE in PBS containing 0.1 mmol L^{-1} L-phenylalanine ($n = 3$). (B) Typical current response curves at the MIP/β-CD–MWNTs/PAN/CE and NIP/β-CD–MWNTs/PAN/CE with increment of concentration L-phenylalanine in PBS; Concentration (mol L^{-1}) of L-phenylalanine: (a) 5.0×10^{-7}, (b) 1.5×10^{-6}, (c) 5.0×10^{-6}, (d) 1.0×10^{-5}, (e) 2.0×10^{-5}, (f) 5.0×10^{-5}, (g) 7.0×10^{-5}, (h) 1.0×10^{-4}, (i) 2.0×10^{-4}, (j) 4.0×10^{-4}, (k) 6.0×10^{-4}, (l) 1.0×10^{-3}. Insert: Calibration curve for the response current at the MIP/β-CD–MWNTs/PAN/CE towards concentration of L-phenylalanine.

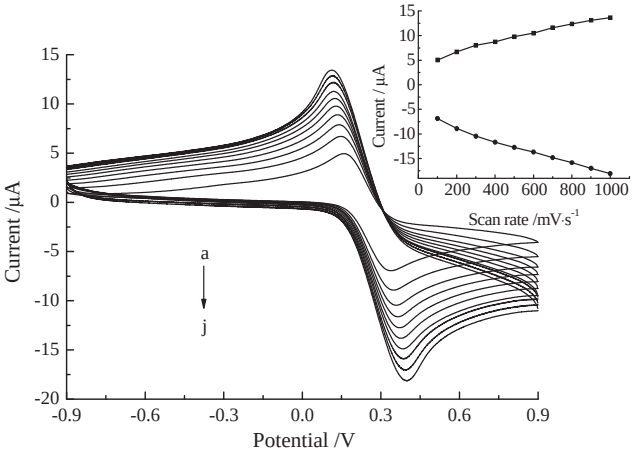

Fig. 7. Cyclic voltammetric responses of MIP/β-CD–MWNTs/PAN/CE in PBS at scan rates; (inner to outer) 100, 200, 300, 400, 500, 600, 700, 800, 900 and 1000 mV s^{-1}; Inset: Plot of peak currents vs. scan rate.

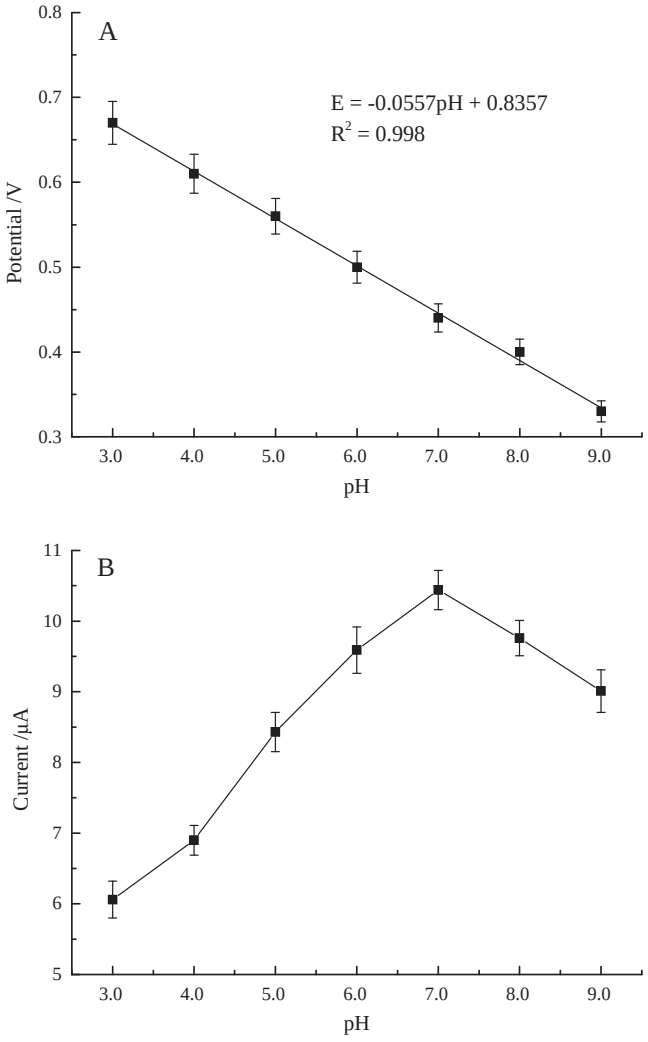

Fig. 8. (A) Calibration plot of pH vs. potential in PBS and (B) the cyclic voltammetry response of the MIP/β-CD–MWNTs/PAN/CE in PBS containing 1.0 mmol L^{-1} L-phenylalanine at different pH values from 3.0 to 9.0; scan rate 50 mV s^{-1}.

and reference electrode, respectively. All potentials were relative to the reference electrode. The surface morphologies of modified electrodes were analyzed by JSM-6700F scanning electron microscope (SEM, Japan).

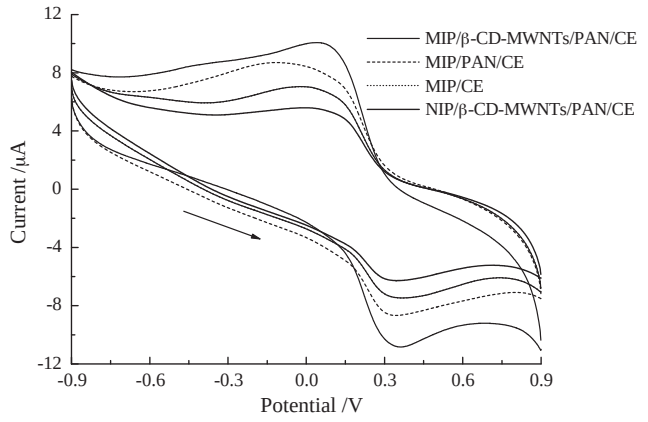

Fig. 9. Cyclic voltammograms for 1.0 mmol L^{-1} L-phenylalanine in blood plasma samples ($n = 3$).

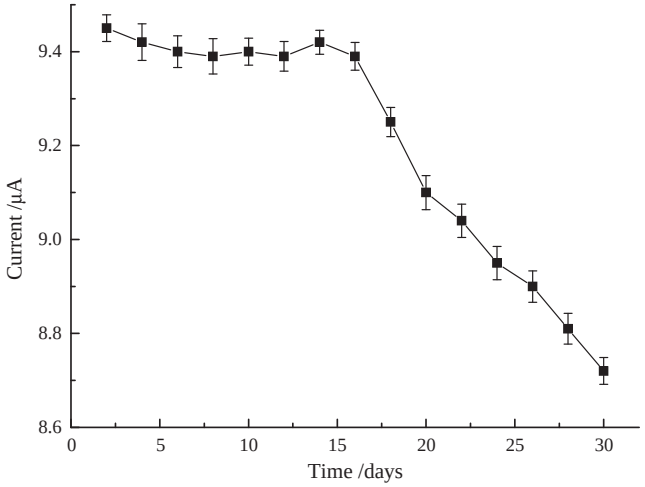

Fig. 10. Reproducibility and stability of the MIP/β-CD–MWNTs/PAN/CE stored in PBS at 25 °C ($n = 3$).

2.3. Carbon electrode pretreatment

First, carbon electrodes (8.0 mm × 5.0 mm) were cleaned using acetone, ethanol and double-distilled water under sonication for 3 min in succession. Then, the carbon electrodes were mechanically polished with 0.3 μm and 0.05 μm alumina slurry to a mirror finish, respectively, rinsed and sonicated in double-distilled water for 1 min. Prior to surface modification, the carbon electrodes were scanned by cyclic voltammetry (CV) from −0.9 to +0.9 V in PBS until repeating cyclic voltammograms appeared. Then, the electrodes were washed with double-distilled water and dried under N_2.

2.4. Fabrication of MIP/β-CD–MWNTs/PAN/CE

The fabrication process of the MIP/β-CD–MWNTs/PAN/CE was shown in Fig. 1. First, crude MWNTs (0.5 g) were added into 60 mL of HNO_3 under sonication for 10 min. Then, the mixture was stirred under 85 °C for 16 h. Cooled to room temperature, the mixture was filtered through a 0.22-μm polycarbonate membrane and washed with double-distilled water for several times until the pH of the filtrate was neutral. The filtered solid was dried with N_2, obtaining carboxylic acid-functionalized MWNTs (MWNTs–COOH). Finally, two milligram of MWNTs–COOH was dispersed with the aid of ultrasonic agitation in 1.0 mL of β-CD aqueous solution (2.0 wt%) for 1 h to give a black suspension.

In the beginning, electrodepositing aniline solution onto the carbon electrode surface to enhance the stability and conductivity was carried out by CV from −0.9 to +0.9 V for 10 cycles at a scan rate of 50 mV s^{-1}. Then, the PAN/CE was immersed into the β-CD–MWNTs suspension for 24 h to obtain a β-CD–MWNTs/PAN/CE.

A total of 3.0 mL of TEOS, 3.0 mL of ethoxyethanol, 0.2 mL of PTMOS, 0.2 mL of MTMOS, 0.5 mL of HCl (0.1 mol L^{-1}) and 3.0 mL of H_2O were mixed and stirred to acquire a homogeneous original sol. Then, 2.0 mL of this sol mixing with 0.3 mL 1.0 mmol L^{-1} of L-phenylalanine solution was stirred for 2 h to obtain an imprinted sol, while the original sol (without L-phenylalanine) was used to prepare non-imprinted reference sol–gel film. Finally, the imprinted or non-imprinted sol was electrodeposited onto the β-CD–MWNTs/PAN/CE surface by using CV from −0.9 to +0.9 V with the scan rate of 50 mV s^{-1} and dried overnight at room temperature. Thus, the imprinted sensor (MIP/β-CD–MWNTs/PAN/CE) and non-imprinted sensor (NIP/β-CD–MWNTs/PAN/CE) were obtained. The doped L-phenylalanine was extracted from the imprinted film by repetitious immersion in PBS, and then air-dried for 24 h.

2.5. Electrochemical measurements

The electrochemical measurements were conducted in 10.0 mL of PBS containing 1.0 mmol L^{-1} L-phenylalanine. The extraction efficiency was investigated by DPV from −0.2 to +1.0 V. The parameters were performed as follows: the pulse amplitude was 50 mV, the pulse width was 50 ms, the pulse period was 200 ms and the potential increment was 4 mV. For amperometric measurement, L-phenylalanine concentration was stepwise increased with an applied potential of +0.4 V at the MIP/β-CD–MWNTs/PAN/CE and NIP/β-CD–MWNTs/PAN/CE. Blood plasma samples were obtained from healthy laboratory volunteers, and used without any pretreatment except that they were diluted by 10 times with PBS. The required quantity of L-phenylalanine was added into the diluted blood plasma solutions were used for voltammetric analysis. All electrochemical experiments were carried out at room temperature.

3. Results and discussion

3.1. Reaction mechanism

L-Phenylalanine-imprinted organic–inorganic film was prepared by sol–gel process in this study. The preparation of organic–inorganic film involved synthesis and gelatin of the precursor sol with the template. The role of the functional organosilane monomers is to assist in this specific recognition rebinding process. Therefore, a specific sol-forming monomers mixture, which consisted of a combination of functional organosilane monomers complementing to its structure and chemical nature, was adjusted to the template molecule. In previous studies [28,29], the results showed the combination of functional monomers can enhance and promote the rebinding of the imprinted film towards the template. TEOS is a non-functionalized silane monomer and its alkoxy groups tend to hydrolyze and polymerize completely to give silanol and siloxanes bonds, which attribute to the hydrophilic/hydrophobic nature of the matrix, respectively. However, TEOS alone cannot create a well-defined matrix for imprinting. In this work, the sol was prepared by combining TEOS and PTMOS (the former allowing for hydrogen bonds and ionic interactions and the latter allowing for σ–σ interactions with the aromatic ring) in ethoxyethanol. Studies showed the relative rates of evaporation and condensation during film deposition affected the pore volume, pore size and surface area of the prepared film [30]. Generally, an increase in evaporation rate gave a compact structure of silica and made the template difficult to remove. Therefore, ethoxyethanol with lower evaporation rate was chosen as the solvent.

3.2. Imprinted sensor preparation and characterization

The electrochemical behavior of aniline was investigated in aqueous solution of 1.0 mol L^{-1} H_2SO_4 using CV between −0.9 and +0.9 V and the results are shown in Fig. 2. Two main pairs of typically reversible redox peaks of PAN are displayed clearly in all curves. The first redox couple at lower positive potential in all curves corresponds to the redox interconversion between leucoemeraldine and emeraldine. The redox couple at the higher potential corresponds to the redox reaction between emeraldine and pernigraniline. As reported previously [31], the first transformation of PAN redox state corresponds to the redox of leucoemeraldine → emeraldine in strongly acidic solutions, only involving the ejection of proton and counter anions in the PAN film, but no anion injection. The following conversion of PAN redox state is the process of emeraldine → pernigraniline, which also involves the ejection of counter anions as well as protons. As shown in Fig. 2, the peak cur-

rents increase in intensity with the scanning time increase because of the redox of the film. However, the peak currents increased slowly. When the scanning time was over 10, the response current curves kept basically unchanged, suggesting a gradual film overlay process. It can be ascribed to the conductivity and self-catalytic properties of polyaniline and illustrated the presence of the complete coverage at the carbon electrode surface.

The modified electrodes were put into the imprinted sol to deposit an imprinted film by CV from −0.9 to +0.9 V at a scan rate of 50 mV s^{-1}. The electrodeposition process was shown in Fig. 3. In the process, the absence of the redox peaks with continuous scanning can be ascribed to form a dense and insulating imprinted sol–gel film on the electrode surface. Thereby the electrode surface area in contact with the solution reduced and the voltammetric responses were suppressed. When the cycle was over 30, the gradually synchronized CV curves were observed, which indicated the electrode surface was covered completely by sol–gel film. Moreover, an increase in the peak current was observed at the MIP/β-CD–MWNTs/PAN/CE compared with the MIP/CE. The results suggested that the β-CD/MWNTs can promote the electrochemical reaction more efficiently and PAN can enhance the conductivity further. Therefore, β-CD/MWNTs and PAN were expected to act as the ideal electrode materials.

The surface morphologies of layer-by-layer modified electrodes were studied by SEM. As presented in Fig. 4, the bare CE surface (Fig. 4A) which displays a smooth surface was covered by PAN film, forming a dense layer (Fig. 4B). The presence of β-CD–MWNTs caused the enhancement of specific surface area (Fig. 4C). Thus can promote electric transfer and enhance the contact area with the analytes. Finally, when the imprinted sol–gel film was electrodeposited, the MIP/β-CD–MWNTs/PAN/CE was fabricated well (Fig. 4D).

Fig. 5A shows the DPV responses of the imprinted film before and after removal of L-phenylalanine in PBS. The peak (+0.4 V) was believed due to the oxidation of L-phenylalanine. After L-phenylalanine removal, the DPV response current of the imprinted film showed significant decrease. This suggested that L-phenylalanine was successfully removed by PBS.

DPV is an effective and convenient technique for probing the feature of the modified electrode surface. Here, DPV was used to investigate electrochemical behaviors for each assembly step. The DPVs of the different modified electrodes in PBS containing 1.0 mmol L^{-1} L-phenylalanine were presented in Fig. 5B. A visible oxidative peak revealed an electrochemical behavior on L-phenylalanine at the MIP/CE (Fig. 5B-a) owing to the formed imprinted binding sites matching with L-phenylalanine. After the MIP/CE was modified with PAN, the peak current increased greatly due to the PAN layer could increase the conductivity for electrical signal (Fig. 5B-b). When the MWNTs were immobilized on the electrode surface, peak current increased in the same way as a result of MWNTs enhancing surface area and active sites for electron transfer (Fig. 5B-c). When the β-CD incorporated MWNTs composite material was formed and covered the electrode surface, the response current added enormously (Fig. 5B-e). This suggested that β-CD incorporated MWNTs can firmly adsorb the template molecule and enhance the electron transfer between redox centers and electrode surface furtherly. But the peak current decreased clearly when PAN was knocked off the system (Fig. 5B-d). Thus, the role of PAN layer enhancing the electrical conductivity of the system was verified. Therefore, β-CD–MWNTs/PAN nanocomposites were used to modify the electrode in this work.

3.3. Electrochemical properties of MIP/β-CD–MWNTs/PAN/CE

The polarization curve of the MIP/β-CD–MWNTs/PAN/CE in 0.1 mmol L^{-1} L-phenylalanine PBS was shown in Fig. 6A. The redox currents approached a limiting current when the applied potential was more positive than +0.4 V. Therefore, the applied potential in this work was set at +0.4 V.

Table 1
Structures of analytes.

Analyte	Structure
L/D-Phenylalanine	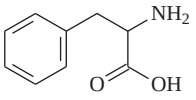
L-Histidine	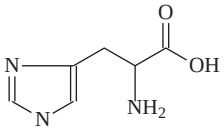
L-Proline	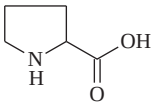
L-Norleucine	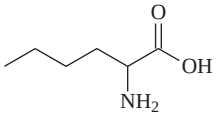
DL-Methionine	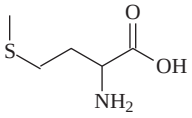

Fig. 6B is the current responses of the MIP/β-CD–MWNTs/PAN/CE and NIP/β-CD–MWNTs/PAN/CE towards L-phenylalanine with concentration ranging from 5.0×10^{-7} to 1.0×10^{-3} mol L^{-1}. As shown in Fig. 6B, the peak current of the MIP/β-CD–MWNTs/PAN/CE was higher than that of NIP/β-CD–MWNTs/PAN/CE at the same L-phenylalanine concentration. This was caused by the absence of imprinted binding sites matching with the template at NIP/β-CD–MWNTs/PAN/CE. The peak current increased with the increment of L-phenylalanine concentration ranging from 5.0×10^{-7} to 1.0×10^{-3} mol L^{-1}. However, the peak current increases slightly when L-phenylalanine concentration was over 1.0×10^{-4} mol L^{-1}. Calibration curve of the peak current of the MIP/β-CD–MWNTs/PAN/CE for L-phenylalanine concentration was observed in the inset of Fig. 6B. The linear relationship between the peak current of the MIP/β-CD–MWNTs/PAN/CE and L-phenylalanine concentration ranging from 5.0×10^{-7} to 1.0×10^{-4} mol L^{-1} was as follows:

$$I = 56.283C + 0.854 \quad (r = 0.971, \quad I \text{ inv}\mu\text{A}, \quad C \text{ in mmol } L^{-1}) \tag{1}$$

The limit of detection (*LOD*) was calculated as 1.0×10^{-9} mol L^{-1} (S/N = 3) [32].

3.4. Selectivity of MIP/β-CD–MWNTs/PAN/CE

To study the selectivity of L-phenylalanine imprinted sensor, some species were chosen as interference based on structural similarity and interaction types. Meanwhile, they appeared usually with L-phenylalanine in human body together. The analytes with molecular structures are listed in Table 1. In this study, to assess the selective recognition performance of the imprinted sensor, selectivity factor (K_{it}), which is defined as the ratio of the sensor's

Table 2
Selectivity factors of sol–gel sensor for substances with structures analogous to that of L-phenylalanine.

Interfering substances	K_{it}[a]	K_{it}[b]	K_{it}[c]
D-Phenylalanine	0.23	1.05	0.87
L-Histidine	0.11	0.97	1.02
L-Norleucine	0.12	0.99	0.99
DL-Methionine	0.10	1.00	1.01
L-Proline	0.09	1.04	0.98

K_{it} presented average of three experiment results.
[a] K_{it} of MIP/β-CD–MWNTs/PAN/CE.
[b] K_{it} of β-CD–MWNTs/PAN/CE.
[c] K_{it} of NIP/β-CD–MWNTs/PAN/CE.

response current shift towards the interfering substance to that towards the template, was calculated. The MIP and NIP sensor were exposed to a series of 1.0×10^{-3} mol L^{-1} interfering substances and the response currents were recorded. As shown in Table 2, the K_{it} towards D-phenylalanine on the imprinted sensor was 0.23, which was less than that on the NIP sensor. The excellent selectivity of the imprinted film was revealed for the discrimination between L-phenylalanine and D-phenylalanine. It is believed that the high selectivity originates from the similarity structure, which differs only in the stereostructures. The K_{it} was 0.11 against L-histidine, which differs from L-phenylalanine by nitrogen heterocyclic. The results indicated that the binding sites can distinguish the small difference from molecule. The imprinted sensor displays higher selectivity against L-norleucine and DL-methionine. The K_{it} of L-norleucine with 0.12 due to the structural difference, even though L-norleucine is smaller in molecular size and contains amino and carboxyl groups. The K_{it} of DL-methionine with 0.10 which has a sulphur atom in hydrocarbon chain was showed at the imprinted sensor. Small K_{it} about 0.09 was observed for L-proline in this work owing to lack of phenyl group, amino and carboxyl groups. However, the NIP sensor did not display selectivity owing to the absence of the binding sites and the nature of prepolymerized complex between the L-phenylalanine and the functional monomers. Furthermore, K_{it} of β-CD–MWNTs/PAN/CE was also presented in Table 2. Similar to NIP sensor, the β-CD–MWNTs/PAN/CE did not display selective recognition ability towards L-phenylalanine.

Some species and ions commonly existing in biological samples involving Na^+, K^+, Mg^{2+}, Ca^{2+}, Cl^- and SO_4^{2-} were chosen to study on the anti-interference effect of the imprinted sensor. The influence of these ions on L-phenylalanine detection was investigated further. The results showed the peak current of 2.0 μmol L^{-1} L-phenylalanine was not affected by 2000-fold of Na^+, K^+, Mg^{2+}, Ca^{2+}, SO_4^{2-} and Cl^-.

3.5. Effect of scan rate

The influence of scan rate on the MIP/β-CD–MWNTs/PAN/CE in PBS was investigated. As shown in Fig. 7, with increasing the scan rate from 100 to 1000 mV s^{-1}, both the cathodic and anodic peak currents increased and their potentials did not considerably shift, indicating a diffusionless, surface-controlled electrode process of L-phenylalanine [33]. According to Laviron equation [34]:

$$I_p = \frac{n^2F^2Av\Gamma}{4RT} = \frac{nFQv}{4RT} \quad (2)$$

where Γ (mol cm^{-2}) is the surface amount of the adsorbed L-phenylalanine on electrode surface, A is the electrode area (cm^2), v is the scan rate, I_p is the peak current, n is the number of electron transferred, Q is the charge involved in the reaction, and F is Faraday's constant. The average surface amount (Γ) of the adsorbed L-phenylalanine on the MIP/β-CD–MWNTs/PAN/CE was estimated to be 8.6×10^{-10} mol cm^{-2}. The result demonstrated the film could considerably increase the functional density of L-phenylalanine.

Since $n\Delta E_p < 200$ mV (E_p: peak potential), the direct electron-transfer rate constant (K_s) of the adsorbed L-phenylalanine on the MIP/β-CD–MWNTs/PAN/CE can be obtained by the following equation [34]:

$$\log K_s = \alpha \log(1-\alpha) + (1-\alpha)\log\alpha - \log\frac{RT}{nFv} - \alpha(1-\alpha)\frac{nF\Delta E_p}{2.3RT} \quad (3)$$

where α is the charge-transfer coefficient, ΔE_p is the peak potential separation, v is the scan rate, n is the number of electron transferred, and F is the Faraday's constant. The results showed the scan rate in the range of 100–1000 mV s^{-1} did not affect the K_s value. Taking the charge-transfer coefficient α of 0.5, at a scan rate of 300 mV s^{-1}, the K_s of the adsorbed L-phenylalanine on the MIP/β-CD–MWNTs/PAN/CE was estimated to be 3.0 s^{-1}. The accelerated electron communication of L-phenylalanine in the present case could be due to the role of electronic wire of β-CD–MWNTs/PAN and the favorable orientation of MIP.

3.6. Effect of pH

The peak potential is closely dependent on the pH of the solution in electrochemical experiment. It was found that the values of peak potential for both peaks at MIP/β-CD–MWNTs/PAN/CE shifted to more negative potentials with the increase of pH (as shown in Fig. 8A) in this study. The plot of peak potentials vs. pH is found to be linear over the pH range of 3.0–9.0 with a slope of 55.7 mV pH^{-1}. This value was close to the expected one of 59 mV pH^{-1} for a single proton-transfer coupled to a reversible single electron transfer at 291 K [35,36]. It suggests the overall process is proton dependent with an equal number of protons and electrons involved in L-phenylalanine redox. The pH value also affected the peak currents of the direct electrochemistry. As shown in Fig. 8B, the maximum peak current at pH 7.0 was obtained in PBS containing 1.0 mmol L^{-1} L-phenylalanine. Therefore, pH 7.0 was used in all electrochemical detection.

3.7. Application

The practical analytical utility of the MIP/β-CD–MWNTs/PAN/CE was assessed by measurement of L-phenylalanine in blood plasma samples without any sample pretreatment. The diluted blood plasma samples were spiked with appropriate amount of L-phenylalanine and the resulting sample was detected by the working-curve method. The adsorbed molecule by the modified electrode was washed with double-distilled water and transferred to PBS before the electrochemical measurement. Fig. 9 shows the cyclic voltammograms obtained for L-phenylalanine redox in blood plasma samples at the MIP/β-CD–MWNTs/PAN/CE, MIP/PAN/CE, MIP/CE and NIP/β-CD–MWNTs/PAN/CE. As shown in Fig. 9, voltammetric signal was observed on the all-modified electrode. However, at the MIP/β-CD–MWNTs/PAN/CE, there are highest voltammetric signal peaks in blood plasma samples, which can be ascribed to the presence of the two functional layers involving β-CD–MWNTs and PAN. Besides, the signal peak at the MIP/CE was lower than that at the MIP/PAN/CE owing to the electrical conductivity and self-catalytic properties of PAN. With lack of imprinted bind sites in non-imprinted film, the voltammetric signal peak at the NIP/β-CD–MWNTs/PAN/CE was lowest.

As a preliminary evaluation of the validity of the proposed electrochemical sensor, the recovery of the L-phenylalanine in blood plasma samples was testified. Varying amounts of L-phenylalanine were added to the diluted (100-fold) blood plasma samples and the results are presented in Table 3. The results showed the imprinted

Table 3
Recoveries of diluted (100-fold) blood plasma samples added with different L-phenylalanine concentrations.

Added (mol L^{-1})	Found (mol L^{-1})	Recovery[a] (%)
1.0×10^{-7}	0.98×10^{-7}	98.0 ± 1.4
2.0×10^{-6}	2.11×10^{-6}	105.5 ± 2.1
4.0×10^{-6}	3.99×10^{-6}	99.8 ± 1.9
8.0×10^{-6}	7.63×10^{-6}	95.4 ± 1.1
2.0×10^{-5}	2.01×10^{-5}	100.5 ± 2.0
4.0×10^{-5}	3.89×10^{-5}	97.3 ± 2.5
8.0×10^{-5}	7.96×10^{-5}	99.5 ± 1.7

[a] Average of three experiment results.

sensor could be used for the determination of L-phenylalanine, with satisfactory recovery results of 95.4–105.5%. The results suggested that the imprinted sensor provided possibilities of clinical application in physiological fluids.

3.8. Reproducibility and stability of MIP/β-CD–MWNTs/PAN/CE

The reproducibility and storage stability of the MIP/β-CD–MWNTs/PAN/CE were investigated by CV to prove the precision and practicability of the proposed method and the results were presented in Fig. 10. The relative standard deviation (RSD) of the modified electrode response to 1.0 mmol L^{-1} L-phenylalanine was 2.9% for ten successive measurements. RSD for determination of 1.0 mmol L^{-1} L-phenylalanine with five sensors prepared under the same conditions was 4.1%. Stored in PBS at 25 °C, the modified imprinted electrode was measured at intervals of 2 days. Before 16 days, no obvious decrease in the currents was observed. The response current of the MIP/β-CD–MWNTs/PAN/CE remained about 92.3% of its original current after 1 month. The excellent reproducibility and stability of the MIP/β-CD–MWNTs/PAN/CE are due to the good compatibility and stability of the MIP layer, β-CD–MWNTs layer and PAN layer. The β-CD–MWNTs layer provides an interconnected three-dimensional matrix for depositing imprinted sol–gel solution. And the response mechanism of β-CD–MWNTs film for L-phenylalanine was based on quick electron transfer of MWNTs and the inclusion interaction of β-CD for L-phenylalanine. The linear range and *LOD* at different MIP sensors were compared with the recently reported chemically modified electrodes and the results are given in Table 4. This revealed a similar order of precision in the results within the concentration range by both methods. The proposed method is simpler, more selective, and cost-effective.

Table 4
Comparison of the present MIP/β-CD–MWNTs/PAN/CE with other MIP sensors.

Different imprinted sensors	Linear range (mol L^{-1})	Detection limit (mol L^{-1})	Reference
Ion imprinted polymer based sensor	2.0×10^{-8} to 1.0×10^{-2}	2.0×10^{-8}	[37]
Para-nitrophenol MIP voltammetric sensor	8.0×10^{-9} to 5.0×10^{-6}	3.0×10^{-9}	[38]
MIP-based electrochemical sensor for monitoring 2,4,6-trinitrotoluene (TNT)	5.0×10^{-9} to 1.0×10^{-6}	1.5×10^{-9}	[10]
A MIP amperometric sensor	2.0×10^{-7} to 3.0×10^{-6}	8.0×10^{-8}	[39]
MIP based potentiometric sensor	1.0×10^{-6} to 1.0×10^{-1}	7.0×10^{-7}	[40]
MIP-based sensor for the detection of chloramphenicol succinate residue	1.0×10^{-8} to 1.2×10^{-5}	2.0×10^{-9}	[41]
MIP/β-CD–MWNTs/PAN/CE	5.0×10^{-7} to 1.0×10^{-4}	1.0×10^{-9}	This work

4. Conclusions

In this study, we have successfully developed a novel and simple fabrication method by combining β-CD–MWNTs composite material with imprinted sol–gel film on the PAN layer modified carbon electrode. The MIP/β-CD–MWNTs/PAN/CE has been applied for sensitive L-phenylalanine detection. The interconnected β-CD–MWNTs composites film and the PAN layer possessed superior conductivity, high stability and excellent electrocatalytic ability and inclusion interaction for the determination of L-phenylalanine. Owing to the presence of imprinted film, the MIP/β-CD–MWNTs/PAN/CE exhibited excellent selectivity towards L-phenylalanine. The MIP/β-CD–MWNTs/PAN/CE has been successfully applied to determine selectively L-phenylalanine in blood plasma samples. Thus, the imprinted sensor provided possibilities of clinical application in physiological fluids.

Acknowledgments

The authors would like to acknowledge financial support from the Nature Science Foundation China (No. 21005030), the Scientific Research Fund of Hunan Provincial Education Department (No. 10A099), the Colonel-level Project of Jishou University of Hunan Province, China (No. 09JDY007) and the Graduate Innovation Foundation of Hunan Province, China (No. CX2010B294).

References

[1] J. Bongaerts, M. Krämer, U. Müller, L. Raeven, M. Wubbolts, Metab. Eng. 3 (2001) 289–300.
[2] H.Y. Zhou, X.Y. Liao, T.W. Wang, G.C. Du, J. Chen, Bioresour. Technol. 101 (2010) 4151–4156.
[3] M.C. Francisco, O. Carmen, M.G. Juan, Neurosci. Lett. 392 (2006) 1–4.
[4] T.T. Liu, S.H. Chiang, S.J. Wu, K.J. Hsiao, Clin. Chim. Acta 313 (2001) 157–169.
[5] P.J. Waters, M. Khashu, Y. Lillquist, C. Senger, A. Mattman, M. Demos, K. Setchell, A. Rupar, P. Scott, N. Blau, H.D. Vallance, Mol. Genet. Metab. 86 (2005) 148–152.
[6] T. Alizadeh, M. Akhoundian, Electrochim. Acta 55 (2010) 3477–3485.
[7] Z.H. Zhang, Y.F. Hu, H.B. Zhang, S.Z. Yao, J. Colloid Interface Sci. 344 (2010) 158–164.
[8] T.A. Sergeyeva, O.A. Slinchenko, L.A. Gorbach, V.F. Matyushov, O.O. Brovko, S.A. Piletsky, L.M. Sergeeva, G.V. Elska, Anal. Chim. Acta 659 (2010) 274–279.
[9] B.B. Prasad, M.P. Tiwari, R. Madhuri, P.S. Sharma, Anal. Chim. Acta 662 (2010) 14–22.
[10] T. Alizadeh, M. Zare, M.R. Ganjali, P. Norouzi, B. Tavana, Biosens. Bioelectron. 25 (2010) 1166–1172.
[11] X.L. Xu, G.L. Zhou, H.X. Li, Q. Liu, S. Zhang, J.L. Kong, Talanta 78 (2009) 26–32.
[12] G.Z. Xie, P. Sun, X.L. Yan, X.S. Du, Y.D. Jiang, Sens. Actuators B: Chem. 145 (2010) 373–377.
[13] M. Joubert, M. Bouhadid, D. Bégué, P. Iratçabal, N. Redon, J. Desbrières, S. Reynaud, Polymer 51 (2010) 1716–1722.
[14] H. Zhang, G.P. Cao, W.K. Wang, K.G. Yuan, B. Xu, W.F. Zhang, J. Cheng, Y.S. Yang, Electrochim. Acta 54 (2009) 1153–1159.
[15] Z.C. Hu, J.J. Xu, Y. Tian, R. Peng, Y.Z. Xian, Q. Ran, L.T. Jin, Electrochim. Acta 54 (2009) 4056–4061.
[16] M.M. Ayad, N.A. Salahuddin, M.O. Alghaysh, R.M. Issa, Curr. Appl. Phys. 10 (2010) 235–240.
[17] J.N. Coleman, U. Khan, W.J. Blau, Y.K. Gun'ko, Carbon 44 (2006) 1624–1652.
[18] F. Simon, H. Kuzmany, Chem. Phys. Lett. 425 (2006) 85–88.
[19] P. Avouris, T. Hertel, R. Martel, T. Schmidt, H.R. Shea, R.E. Walkup, Appl. Surf. Sci. 141 (1999) 201–209.
[20] S. Iijima, Nature 354 (1991) 56–58.
[21] A. Salimi, R.G. Compton, R. Hallaj, Anal. Biochem. 333 (2004) 49–56.
[22] J. Wang, S.B. Hocevar, B. Ogorevc, Electrochem. Commun. 6 (2004) 176–179.
[23] J.M. Nugent, K.S.V. Santhanam, A. Rubio, P.M. Ajayan, Nano Lett. 1 (2001) 87–91.
[24] K.P. Gong, Y. Dong, S.X. Xiong, Y. Chen, L.Q. Mao, Biosens. Bioelectron. 20 (2004) 253–259.
[25] J. Wang, M. Musameh, Anal. Chim. Acta 511 (2004) 33–36.
[26] Y. Xu, Y. Jiang, H. Cai, P.G. He, Y.Z. Fang, Anal. Chim. Acta 516 (2004) 19–27.
[27] J.L. He, Y. Yang, X. Yang, Y.L. Liu, Z.H. Liu, G.L. Shen, R.Q. Yu, Sens. Actuators B 114 (2006) 94–100.
[28] S. Marx, Z. Liron, Chem. Mater. 13 (2002) 3624–3630.
[29] S. Marx, A. Zaltsman, I. Turyan, D. Mandler, Anal. Chem. 76 (2004) 120–126.
[30] C.J. Brinker, G.W. Scherer, Sol–Gel Science, Academic Press, Boston, 1990, p. 797.
[31] E. Salamifar, M.A. Mehrgardi, M.F. Mousavi, Electrochim. Acta 54 (2009) 4638–4646.
[32] H.Y. Xiang, W.G. Li, Electroanalysis 21 (2009) 1207–1210.

[33] H.C. Yoon, M.Y. Hong, H.S. Kim, Anal. Chem. 72 (2000) 4420–4427.
[34] E. Laviron, J. Electroanal. Chem. 100 (1979) 263–270.
[35] A.E.F. Nassar, Z. Zhang, N.F. Hu, J.F. Rusling, J. Phys. Chem. B 101 (1997) 2224–2231.
[36] X. Chen, N. Hu, Y. Zeng, J.F. Rusling, J. Yang, Langmuir 15 (1999) 7022–7030.
[37] P. Metilda, K. Prasad, R. Kala, J.M. Gladis, T. Prasada Rao, G.R.K. Naidu, Anal. Chim. Acta 582 (2007) 147–153.
[38] T. Alizadeh, M.R. Ganjali, P. Norouzi, M. Zare, A. Zeraatkar, Talanta 79 (2009) 1197–1203.
[39] Y. Liu, Q.J. Song, L. Wang, Microchem. J. 91 (2009) 222–226.
[40] M. Javanbakht, S.E. Fard, A. Mohammadi, M. Abdouss, M.R. Ganjali, P. Norouzi, L. Safaraliee, Anal. Chim. Acta 612 (2008) 65–74.
[41] N.W. Zhang, M.X. Ding, G.Y. Liu, W.W. Song, C.Y. Chai, Chin. J. Anal. Chem. 36 (2008) 1380–1384.